UNIVERSIDAD TECNOLÓGICA METROPOLITANA del Estado de Chile
UTEM

REVISTA MMSB

Revista de Modelamiento Matemático de Sistemas Biológicos
https://revistammsb.utem.cl | revista.mmsb@utem.cl
Vol.3(2023), No.2, pp.1–19, e23R05
ISSN-L: 2735-6817 | ISSN (online): 2735-6817
https://doi.org/10.58560/rmmsb.v03.n02.023.08

Estrategias de búsqueda y defensa inducidas por quimiotaxis en un sistema tritrófico

Chemotactically induced search and defense strategies in a tritrophic system

Néstor Anaya[1,2], Manuel Falconi [1] and Guilmer Ferdinand González Flores[1]

✉ Néstor Anaya: nianayao@uaemex.mxl

[1] Departamento de Matemáticas, Facultad de Ciencias,
Universidad Nacional Autónoma de México
Ciudad de México, México

[2] Departamento de Matemáticas, Facultad de Ciencias,
Universidad Autónoma del Estado de México,
Toluca, México

Recepción: 2023-06-14 | Aceptación: 2023-10-30 | Publicación: 2023-12-29

Recommended Citation: Anaya, N. *et al.* (2023). *'Estrategias de búsqueda y defensa inducidas por quimiotaxis en un sistema tritrófico'*. Rev. model. mat. sist. biol. 3(2), e23R05, doi:10.58560/rmmsb.v03.n02.023.08

Support: PAPIIT IA203922

ABSTRACT

In this paper, we define an intraguild predation model of one-resource and two-predator, in which the mesopredator catched by a top predator, feeds on a resource that grows according to a logistic growth law; for both the meso and the top predator, Holling type II functional responses are considered. Predators and prey diffuse into a connected bounded region in $\mathbb{R}^2$. Two scenarios are considered: 1. As a defense mechanism, the resource attracts the top predator that feeds on the mesopredator; 2. The top predator in search of food moves towards areas where the mesopredator population is increasing. Some general properties of the solutions of the model are proved. In addition, the results of the numerical simulations carried out to analyze the effect on the spatial distribution of the populations of the indirect defense mechanism of the first scenario are shown. This is contrasted with the results of the model simulations corresponding to the second scenario, in which the diffusion of the top predator is regulated by a tendency to move towards the mesopredator gradient.

Keywords:

Competing species; Intraguild predation; Chemotaxis, Active-search hunting

RESUMEN

En este trabajo se define un modelo de depredación intragremial de un recurso y dos depredadores, en el cual el recurso crece de acuerdo a una ley de crecimiento logístico y es el alimento de un mesodepredador que es capturado por el depredador principal; para ambas clases de depredadores se considera una respuesta funcional Holling tipo II. Depredadores y presas se difunden en una región conexa y acotada de $\mathbb{R}^2$. Se estudian dos escenarios: 1) El recurso atrae, como un mecanismo de defensa, al depredador principal que se alimenta del mesodepredador; 2) En la búsqueda de alimento, el depredador principal se mueve hacia las áreas donde es creciente la población del mesodepredador. Se demuestran algunas propiedades generales de las soluciones del modelo. Además, se realizan simulaciones numéricas para analizar los efectos sobre la distribución espacial de las poblaciones, del mecanismo de defensa indirecta del primer escenario. Esto es confrontado con los resultados de la simulaciones del modelo correspondiente al segundo escenario, en el que la difusión del depredador principal está regulada por su tendencia a moverse hacia el gradiente del mesodepredador.

Palabras Claves:

Competencia de especies; Depredación intragremial; Quimiotaxis; Cazador de búsqueda activa

2020 AMS Mathematics Subject Classification: Primary: 92B05; Secondary:

1 INTRODUCTION

Individual movement regulated by concentrations of chemical substances is a very frequent natural phenomenon; known as *Chemotaxis* is an important mechanism, for instance, of bacterial populations in search of nutrients or to establish symbiotic relationships (see (Raina *et al.*, 2019)). Chemical components has been observed as a defense strategy of several species. In (Pereira *et al.*, 2000), the authors review some recent studies focused on characterizing the so-called plant volatiles induced by herbivores and the olfactory mechanisms present in some tritrophic interactions. The way in which organisms respond to chemotaxis has been discussed in (Iino and Yoshida, 2009). In particular, it describes the movements that *C. elegans* makes when the NaCl concentration decreases. In this paper it is mentioned that *C. elegans* rapidly changes the direction of locomotion through the use of a set of stereotyped behaviors, in response to a decrease in the concentration of the chemical substance. To get some insight of the impact of chemotactic processes on the population dynamics of some species, (Pereira *et al.*, 2000) studied the chemical defense of two species of brown alga *Dictyota menstrualis* and *Dictyota mertensii* used against herbivores with limited mobility, the amphipod *Parhyale hawaiensis* and the crab *Pachygrapsus transversus*. In fact, natural defense against predation is very well documented and it is present in both invertebrate and vertebrate species, see (Dumbacher and Pruett-Jones, 1996), (Eisner *et al.*, 2000), (Fattorini *et al.*, 2010), (Matz *et al.*, 2008), (Buonomo *et al.*, 2019). On the other hand, the study about the relationship of organism dispersal and community structure of interacting species has a long history. Since the works of Kolmogorov (Kolmogorov, 1937) and Skellam (Skellam, 1951), mathematical modeling of diffusion and random walk has been widely applied in the study of the effect of individual movement on the dynamic properties of different kinds of species interaction. Among the recent works on this topic it is (Yang and Fu, 2008) where the authors consider a tritrophic food chain with predators and one resource; the existence and boundedness of solutions and stability of equilibrium solutions are analyzed. Stability and Turing patterns of a diffusive predator-prey model have been analyzed in (Song *et al.*, 2020). Diffusion and delay effect has been incorporated in an intraguild predation model in (Han and Dai, 2017), where the authors studied how the delay on the conversion rate of mesopredator induces spatiotemporal patterns. About diffusion in predator-prey context see (Venturino and Petrovskii, 2013) and (Ai *et al.*, 2017). In this work we analyzed how the emission of chemical substances which attract predators of consumers of a resource impacts the spatial distribution of species. A laboratory study on this topic is (Kessler and Baldwin, 2001) where Kessler and Baldwin have found that volatile emissions from *Nicotiana attenuata* could reduce the number of herbivores up to 90%.

In this work, we consider an intraguild predation model of one resource and two predators; the importance of this interaction for population ecology has been explained by Polis and Holt in (Polis and Holt, 1992). We consider that mesopredator feed on a resource which grows acoording to a logistic growth law and it is consumed by a top predator; functional responses of meso and top predators are of Holling type II. Predators and prey difusse in a connected bounded region $\Omega \subset \mathbb{R}^2$ of the plane whose boundary $\partial\Omega$ is a regular curve. We consider two cases: in the first case, the model is

$$\begin{aligned} \frac{\partial u}{\partial t} &= d_0\Delta u + \alpha u\left(1-\frac{u}{K}\right) - \frac{buv}{u+a}, \\ \frac{\partial v}{\partial t} &= d_1\Delta v + \gamma\frac{buv}{u+a} - \frac{cvw}{v+d} - \mu v, \\ \frac{\partial w}{\partial t} &= d_2\Delta w + \beta\frac{cvw}{v+d} - \rho w - \nabla\cdot\left(\chi_1(v,w)\nabla v\right), \end{aligned} \tag{1}$$

the random dispersal of top predators is tempered by a certain tendency to move up the gradient of mesopredators. Pheronomes have been reported (see (Yoshimizu *et al.*, 2018)) to affect foraging behavior in such a way that the individual chemotactic response is modulated by interactions with other organisms in the population. For this reason, the chemotactic sensitivity $\chi_1(v,w)$ depends on w.

In the second case, as a chemotactic defense mechanism of the prey is considered, the resource population attracts top predators which feeds on mesopredator; this kind of indirect defense against predators has been reported in (Aljbory and Chen, 2018), see also (Buonomo *et al.*, 2019); 2) top predator in search of food moves towards areas where the mesopredator population is increasing The model is given by

$$\begin{aligned} \frac{\partial u}{\partial t} &= d_0\Delta u + \alpha u(1-\frac{u}{K}) - \frac{buv}{u+a}, \\ \frac{\partial v}{\partial t} &= d_1\Delta v + \gamma\frac{buv}{u+a} - \frac{cvw}{v+d} - \mu v, \\ \frac{\partial w}{\partial t} &= d_2\Delta w + \beta\frac{cvw}{v+d} - \rho w - \nabla\cdot(\chi_2(u,w)\nabla u), \end{aligned} \tag{2}$$

in this model the random movement is regulated by the gradient of population density of the resource. In the above models, the carrying capacity $K = K(x,y)$ is a non-negative function defined in Ω and describes the diverse suitability of the niche of the resource. Niche suitability and size population has been addressed in (Osorio-Olvera and Falconi, 2019). It is assumed that the flux vanishes in the boundary of Ω,

$$\frac{\partial u}{\partial \eta}(x,t) = \frac{\partial v}{\partial \eta}(x,t) = \frac{\partial w}{\partial \eta}(x,t) = 0, x \in \partial\Omega, t > 0 \tag{3}$$

where $\partial/\partial\eta = \eta\cdot\nabla$, and η is the normal vector to $\partial\Omega$.
The intrinsic growth of the resource u is denoted by α; b and c are the mortality rate by predation on u and v, respectively. The conversion rate of biomass captured by v and w are γ and β, respectively. The parameters μ and ρ stand for the mortality rate of meso and top predators, respectively. The half saturation constant a estimates the handling time of prey by predators. In Model (1) it is assumed that the regulating mechanism against of random dispersal of w depends

doi: 10.58560/rmmsb.v03.n02.023.08

on a volatile substance generated by v; in Model (2), it is generated by u. Two predators which feed on a common resource subject to a Lotka-Volterra interaction was considered in (Wang *et al.*, 2017), where it was assumed that diffusive movement of predators is controlled by the prey density gradient. In (Tello and Wrzosek, 2016) was analyzed a predator-prey model where predator moves toward the gradient of a chemical released by prey.
The underlying ordinary differential system corresponding to Models (1) and (2) is given by

$$\begin{aligned} u' &= \alpha u\left(1-\frac{u}{K}\right)-\frac{buv}{u+a}, \\ v' &= \gamma\frac{buv}{u+a}-\frac{cvw}{v+d}-\mu v, \\ w' &= \beta\frac{cvw}{v+d}-\rho w. \end{aligned} \tag{4}$$

The system (4) has the following equilibrium points

i) $P_1=(0,0,0)$

ii) $P_2=(K,0,0)$

iii) $P_3=\left(\frac{a\mu}{b\gamma-\mu},\frac{a\alpha\gamma(b\gamma K-\mu(a+K))}{K(b\gamma-\mu)^2},0\right)$.

Under appropriate conditions, this system posses one equilibrium point $P_4=(u_1,v_1,w_1)$ with positive coordinates given by

$$\begin{aligned} u_1 &= \tfrac{1}{2}\left(-a+K+\sqrt{\frac{c\alpha\beta(a+K)^2-\left(4bdK+(a+K)^2\alpha\right)\rho}{(c\beta-\rho)\alpha}}\right) \\ v_1 &= \frac{d\rho}{c\beta-\rho} \\ w_1 &= \frac{(d+v_1)\left(b\gamma u_1-(a+u_1)v_1\mu\right)}{c\left(a+u_1\right)} \end{aligned}$$

Point P_1 is always unstable; P_2 is locally asymptotically stable if $bK\gamma-a\mu-K\mu<0$ and unstable if $bK\gamma-a\mu-K\mu>0$; P_3 is stable if $bK\gamma-a\mu-K\mu>0$ and $b\gamma a>bK\gamma-a\mu-K\mu$ and unstable if $bK\gamma-a\mu-K\mu>0$ and $b\gamma a<bK\gamma-a\mu-K\mu$.

2 EXISTENCE OF POSITIVE SOLUTION

In this section we provide conditions for the existence of positive solutions of systems (1) and (2) for the initial conditions

$$t=0\text{: } u=u_0(x),\ v=v_0(x),\ w=w_0(x),\ x\in\Omega \tag{5}$$

and the boundary conditions given by (3). Let $p>n\geq 1$; then $W^{1,p}(\Omega,\mathbb{R}^n)$ is continuously embedded in the continuous function space $C(\Omega;\mathbb{R}^n)$. Let

$$X:=\{y\in W^{1,p}(\Omega,\mathbb{R}^3)\,|\,\eta\cdot\nabla y_{|_{\partial\Omega}}=0\}.$$

It is assumed that there exist $0<\varepsilon_m$, ε_M, such that

$$\varepsilon_m<K(x,y)<\varepsilon_M,\ \text{for all}(x,y)\in\Omega \tag{6}$$

Theorem 1 *If $(u_0,v_0,w_0)\in X$, then*

(i) There exists $T=T_{\max}\in[0,\infty)$, which depends on the initial conditions (5) such that the problem (1),(3)and (5) has a unique maximal solution $(u,\ v,\ w)$ on $\Omega\times[0,T_{\max})$ and $(u(\cdot,t),\ v(\cdot,t),\ w(\cdot,t))\in C((0,\ T_{\max}),\Omega)$, $(u,v,w)\in C^{2,1}\left((0,T_{\max})\times\overline{\Omega},\mathbb{R}^3\right)$;

(ii) If $u_0,\ v_0,\ w_0\geq 0$ on $\overline{\Omega}$, then $u,\ v,\ w\geq 0$ on $\Omega\times[0,T_{\max})$;

(iii) If $\|(u,w,w)(\cdot,t)\|_{L^\infty(\Omega)}$ is bounded for all $t\in[0,T_{\max})$, then $T_{\max}=+\infty$; equivalently, (u,v,w) is a global solution.

Proof Let $z=(u,v,w)\in\mathbb{R}^3$. Then, (1),(3) and (5) can be written as

$$\begin{aligned} z_t &= \nabla\cdot(A(z)\nabla z)+F(z)\ \text{on}\ \Omega\times[0,\infty) \\ B_z &= \frac{\partial}{\partial\eta}z=0\ \text{on}\ \partial\Omega\times[0,\infty) \\ z(\cdot,0) &= (u_0,v_0,w_0)\ \text{en}\ \Omega, \end{aligned} \tag{7}$$

where

$$A[z]=\begin{bmatrix} d_0 & 0 & 0 \\ 0 & d_1 & 0 \\ 0 & -\chi_1 & d_2 \end{bmatrix}$$

and

$$F(z)=\begin{bmatrix} u\left(\alpha\left(1-\frac{u}{K}\right)-\frac{bv}{u+a}\right) \\ v\left(\gamma\frac{bu}{u+a}-\frac{cw}{v+d}-\mu\right) \\ w\left(\beta\frac{cv}{v+d}-\rho\right) \end{bmatrix}$$

Matrix $A[z]$ is triangular, then the eigenvalues are the diagonal entries d_0, d_1 and d_2, which are assumed to be positive, then the systen (7) is normally elliptic, see pages 15-16 of (Amann, 1990). The result follows from (Haskell and Bell, 2020). □

According to the above theorem, to prove the existence of global solutions it is necessary to show that u, v and w are uniformly bounded in $L^\infty(\Omega)$.

Theorem 2 *If $(u_0,v_0,w_0)\in X$, then the solutions of the System (1), with boundary conditions (3) and initial conditions (5) are bounded.*

doi: 10.58560/rmmsb.v03.n02.023.08

Proof Let $W(x,t) = u + \frac{1}{\gamma}v + \frac{1}{\gamma\beta}w$, so

$$\begin{aligned}
\frac{d}{dt}\int_\Omega (W(x,t)) &= \int_\Omega \left(d_0\Delta u + \alpha u\left(1-\frac{u}{K}\right) - \frac{buv}{u+a}\right)dx \\
&+ \int_\Omega \left(\frac{1}{\gamma}\left(d_1\Delta v\right)\right)dx \\
&+ \int_\Omega \left(\frac{1}{\gamma}\left(\gamma\frac{buv}{u+a} - \frac{cvw}{v+d} - \mu v\right)\right)dx \\
&+ \int_\Omega \left(\frac{1}{\gamma\beta}\left(d_2\Delta w + \beta\frac{cvw}{v+d} - \rho w\right)\right)dx \\
&- \int_\Omega \left(\frac{1}{\gamma\beta}\left(\nabla\cdot\left(\chi_1(v,w)\nabla v\right)\right)\right)dx \\
&= \int_\Omega \left(d_0\Delta u + \frac{1}{\gamma}d_1\Delta v + \frac{1}{\gamma\beta}d_2\Delta w\right)dx \\
&+ \int_\Omega \left(\alpha u\left(1-\frac{u}{K}\right)\right)dx \\
&+ \int_\Omega \left(-\frac{buv}{u+a} + \frac{buv}{u+a} - \frac{c}{\gamma}\frac{vw}{v+d}\right)dx \\
&+ \int_\Omega \left(-\frac{\mu}{\gamma}v + \frac{c}{\gamma}\frac{cvw}{v+d} - \frac{\rho}{\gamma\beta}w\right)dx \\
&\leq \int_\Omega \left(\alpha u\left(1-\frac{u}{K}\right) - \frac{\mu}{\gamma}v - \frac{\rho}{\gamma\beta}\right)dx
\end{aligned}$$

It follows that

$$\frac{d}{dt}\int_\Omega W dx + \int_\Omega \left(\frac{\mu}{\gamma}v + \frac{\rho}{\gamma\beta}w\right)dx \leq \int_\Omega \alpha u\left(1-\frac{u}{K}\right)dx. \tag{8}$$

On the other hand, let $\mu_0 = \min\{\mu,\rho\}$ that implies

$$\frac{d}{dt}\int_\Omega W dx + \mu_0\int_\Omega \left(\frac{1}{\gamma}v + \frac{1}{\gamma\beta}w\right)dx \leq \frac{d}{dt}\int_\Omega W dx + \int_\Omega \left(\frac{\mu}{\gamma}v + \frac{\rho}{\gamma\beta}w\right)dx. \tag{9}$$

From (8) and (9), we obtain that

$$\frac{d}{dt}\int_\Omega W dx + \mu_0\int_\Omega \left(u + \frac{1}{\gamma}v + \frac{1}{\gamma\beta}w\right)dx \leq \int_\Omega \left(\alpha u\left(1-\frac{u}{K}\right)\right)dx + \int_\Omega \mu_0 u dx \tag{10}$$

Note that

$$\begin{aligned}
\int_\Omega \left((\alpha+\mu_0)u - \frac{\alpha u^2}{K}\right)dx &\leq \\
\int_\Omega \frac{1}{4}\frac{K(\alpha+\mu_0)^2}{\alpha}dx &\leq \\
\frac{1}{4}\frac{\varepsilon_M(\alpha+\mu_0)^2}{\alpha}|\Omega| &
\end{aligned} \tag{11}$$

Now, let $K_0 = \frac{1}{4}\frac{\varepsilon_M(\alpha+\mu_0)^2}{\alpha}|\Omega|$, then from (10) and (12) we have that

$$\frac{d}{dt}\int_\Omega W dx + \mu_0\int_\Omega \left(u + \frac{1}{\gamma}v + \frac{1}{\gamma\beta}w\right)dx \leq K_0$$

from this, is clearly evident that

$$\int_\Omega \left(u + \frac{1}{\gamma}v + \frac{1}{\gamma\beta}w\right)dx \leq K_0 + ce^{-t}$$

It follows that solutions are bounded, since according to Theorem 1.(ii), u,v,w are nonegative. □

The proof of the following theorem is similar to those of Theorem 1.

Theorem 3 *Let* $(u_0,v_0,w_0) \in X$.

- *There exists* $T = T_{\max} \in [0,\infty)$, *which depends on the initial conditions (5) such that the problem (2),(3) and (5) has a unique maximal solution* $(u,\ v,\ w)$ *on* $\Omega \times [0,T_{\max})$ *and* $(u(\cdot,t),\ v(\cdot,t),\ w(\cdot,t)) \in C((0,\ T_{\max}),\Omega)$, $(u,v,w) \in C^{2,1}\left((0,T_{\max})\times\overline{\Omega},\mathbb{R}^3\right)$;
- *If* $u_0,\ v_0,\ w_0 \geq 0$ *on* $\overline{\Omega}$, *then* $u,\ v,\ w \geq 0$ *on* $\Omega\times[0,T_{\max})$;
- *If* $\|(u,w,w)(\cdot,t)\|_{L^\infty(\Omega)}$ *is bounded for all* $t \in [0,T_{\max})$, *then* $T_{\max} = +\infty$; *i.e.,* (u,v,w) *is a globally bounded solution.*

Note that v and w vanish if $\gamma b \leq \mu$ and $\beta c \leq \rho$, respectively. From now on, we assume that $\gamma b > \mu$ and $\beta c > \rho$.

Let $Y = \left\{U = (u,v,w) \in \left[C^1\left(\overline{\Omega}\right)\right]^3 | \partial_\rho u(x) = 0,\ x \in \partial\Omega\right\}$, and μ_i be the eigenvalues of the operator $-\Delta$ on Ω with the homogeneous Neumann boundary condition. We denote by $E(\mu_i)$, the eigenspace corresponding to μ_i in $C^1\left(\overline{\Omega}\right)$. let

$$\left\{\phi_{i,j},\ j = 1,2,...,\dim(E(\mu_i))\right\}$$

be a orthonormal basis of $E(\mu_i)$ and $Y_{ij} = \left\{C\cdot\phi_{ij} | C \in \mathbb{R}^3\right\}$. Then,

$$Y_i = \oplus_{j=1}^{\dim(E(\mu_i))} Y_{ij}, Y = \oplus_{i=1}^{\infty} Y_i.$$

Theorem 4 *Let* $0 < K \in \mathbb{R}$. *If* $bK\gamma - a\mu - K\mu < 0$ *then the equilibrium point* P_2 *of system (1) is asymptotically stable.*

Proof Let $A[z] = \begin{pmatrix} d_0 & 0 & 0 \\ 0 & d_1 & 0 \\ 0 & -\chi_1 & d_2 \end{pmatrix}$ as in theorem 1 and $L = A[z]\Delta + J_1$ where J_1 is the Jacobian matrix of the system without diffusion evaluated at P_2; i.e.

$$J_1 = \begin{pmatrix} -\alpha & -\frac{bK}{a+K} & 0 \\ 0 & \frac{bK\gamma}{a+K} - \mu & 0 \\ 0 & 0 & -\rho \end{pmatrix}.$$

The linearization of the system at P_2 is $U_t = LU$. Y_i is invariant with respect to operator L for all $i \geq 1$; λ is an eigenvalue of L restricted to Y_i if and only if is an eigenvalue of matrix $-\mu_i A[z]\Delta + J_1$.

The characteristic polynomial of $\mu_i A[z]\Delta + J_1$ is

$$\varphi_i(\lambda) = (\lambda + \mu_i d_1 + \alpha)\left(\lambda + \mu_i d_2 - \frac{bK\gamma}{a+K} + \mu\right)(\lambda + \mu_i d_2 + \rho)$$

whose roots are $-\mu_i d_1-\alpha$, $-\mu_i d_2+\frac{bK\gamma}{a+K}-\mu$ and $-\mu_i d_2-\rho$. Therefore, the point-spectrum of L consists of eigenvalues that satisfy $\{\mathrm{Re}\,\lambda \leq -(1/2)\max\{\alpha, -\frac{bK\gamma}{a+K}+\mu,\rho\}\}$ whenever $bK\gamma - a\mu - K\mu < 0$; from which stability around P_2 follows, [(Henry, 2006),Th. 5.1.1]. □

The spatial discretization that we apply to perform some numerical simulations of the previous models are describes in the Appendix. In the following computations we apply the finite element method with a time step $\Delta t = 0.001$ and the mesh is conformed by 17385 vertices, 34288 triangles and $h_{\min} = 0.0117835$. $h_{\max} = 0.028418$.

3 NUMERICAL SIMULATIONS

In this section, some numerical simulations are carried out in order to obtain some knowledge about the effect on the population density of the indirect defense mechanism of the resource against the meso–predator, which consists on the attraction of the main predator towards the resource. This will be contrasted with the results of the corresponding simulations of Model (1), in which the random diffusion of the main predator is regulated by a tendency to move towards the gradient of the meso-predator; this is the case of predators actively searching for prey, see (Ioannou and Krause, 2008), (Ross and Winterhalder, 2015) and the references cited there.

MODEL 1: ACTIVE-SEARCH HUNTING.

In the following we consider Model (1) where the top predator is an active-search hunter. We take

$$\chi_1(v,w) = e_1 w - e_2 v.$$

Therefore the top predator move towards the gradient of mesopredator only if its population density is large enough compared to that of the mesopredator. The ratio $\frac{e_2}{e_1}$ measures the defensive capacity of the mesopredator in terms of its population size; the larger this ratio, the greater the density of the predator required to advance towards the prey. The parameter values are given by $\alpha = 5, a = 2.0, b = 5.0, c = 0.1, d = 2.0, \beta = 1.0, \gamma = 1.0, \mu = 0.05, \rho = 0.05, d_0 = 0.1, d_1 = 1, d_2 = 1$.

For this parameter values, the equilibrium points of system (4) are $P_1 = (0,0,0)$, $P_2 = (K,0,0)$, $P_3 = (\frac{2}{99}, \frac{200(99K-2)}{9801K}, 0)$. Existence and stablity properties of these equilibrium points are described in Table 1. Notice that there is no CEP point for the above parameter values. For the numerical computations we assume that $\Omega = [-1,1]\times[-1,1]$ and we have used the `FreeFem++` software (Hecht, 2012). Initial conditions for the spatial distribution of the resource, the meso-predator and top predator are considered as

$$\begin{aligned} u_0(x,y) &= 2\exp(-10(x^2+(y-.9)^2))(1-x^2)^2(1-y^2)^2; \\ v_0(x,y) &= 2\exp(-(x+.9)^2-(y+.9)^2)(1-x^2)^2(1-y^2)^2; \\ w_0(x,y) &= 1.5 \end{aligned}$$

for all $x,y \in \Omega$. In contrast with the meso predator and the resource, the top predator is initially uniformly distributed, (see Figure 1).

Table 1

Point	Existence Interval	Stable	Unstable
P_1	$K>0$		$K>0$
P_2	$K>0$	$K<\frac{2}{99}$	$K>\frac{2}{99}$
P_3	$K>\frac{2}{99}$	$\frac{2}{99}<K<\frac{202}{99}$	$K>\frac{202}{99}$
P_4	$K>\frac{200}{99}$		$K>\frac{200}{99}$

Defensive capacity and species distribution

We consider five different defensive capacities of the prey. The suitability of the habitat of the resource is given by

$$\begin{aligned} K(x,y) &= 2\exp(-5((x+.75)^2+(y-.75)^2)) \\ &\quad +2\exp(-5((x-.75)^2+(y+.75)^2)) \\ &\quad +2\exp(-5((x+.75)^2+(y+.75)^2)) \\ &\quad +2\exp(-5((x-.75)^2+(y-.75)^2)). \end{aligned}$$

Notice that the range of K in Ω is contained in the interval $(\frac{2}{99}, \frac{200}{99})$. Therefore, according to Table 1 system 4 without diffusion does not have the coexistence point P_4 and also the point P_3 is asymptotically stable. Thus, without diffusion the top predator w would become extinct.

First, let $e_1 = 1.0, e_2 = 1.0$. In this case, the defensive capacity of the prey is neutral. Top predator move towards mesopredator whenever its density be greater than the one of the mesopredator

Second, let $e_1 = 1.0, e_2 = 0.5$ In this case, the mesopredator defense against of top predator is lesser than the above case. Thus, we observe that predators are closer to the mesopredators than in the first case (see Figures 2 and 6).

Third, let $e_1 = 1.0, e_2 = 2.0$. Prey presents a strong defense capacity. Notice that predators tends to move towards the lower density areas of the prey population, (see Figures 2 and 3).

Fourth case, let $e_1 = 1.0, e_2 = 10.0$. Prey presents still a defense capacity stronger than the previous case.

Fifth case, Let $e_1 = 10.0, e_2 = 1.0$ This is the smallest defensive capacity considered in this section.

From the comparison of Figures 6-5, we conclude that defensive capacity has a negligible effect on the prey population, if the predation rate is not large enough. Indeed, the main impact is over the spatial distribution of both the meso predator and the top predator.

Habitat suitability and species distribution

To understand how the ecological landscape impact species distribution, we consider two different characterization of the carrying capacity. In either case, the values of parameters of χ_1 are $e_1 = 1.0, e_2 = 10.0$, and the initial condition of u is

$$u_0(x,y) = 2\exp(-10(x^2+y^2))(1-x^2)^2(1-y^2)^2$$

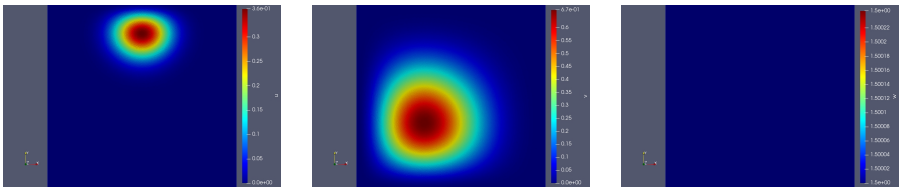

$(a_1)\ u, \quad t=0$ $(b_1)\ v, \quad t=0$ $(c_1)\ w, \quad t=0$

Figure 1: *Contour plots* of time evolution of the resource u, mesopredador v and top predador w at different times.

The initial conditions $v_0(x,y)$ and $w_0(x,y)$ are the same as above.
First, we consider a carrying capacity given by

$$\begin{aligned} K(x,y) &= 2\exp(-5((x+.75)^2+(y-.75)^2)) \\ &\quad +2\exp(-5((x-.75)^2+(y+.75)^2)) \\ &\quad +2\exp(-5((x+.75)^2+(y+.75)^2)) \\ &\quad +2\exp(-5((x-.75)^2+(y-.75)^2)). \end{aligned}$$

The highest suitability is reached at four symmetrical points respect to the origin.

In Figure 7 are shown plots of the numerical solutions of u, v and w at different times. Note that as time passes, the resource tends to occupy the most suitable sites. The mesopredator moves towards the sites with the higher resource density and its defensive capacity (e_2/e_1) is large enough to keep the top predator away.

In this second case, the habitat of the resource is richer since its suitability is given by

$$\begin{aligned} K(x,y) &= 2\exp(-5((x+.75)^2+(y-.75)^2)) \\ &\quad +2\exp(-5((x-.75)^2+(y+.75)^2)) \\ &\quad +2\exp(-5((x+.75)^2+(y+.75)^2)) \\ &\quad +2\exp(-5((x-.75)^2+(y-.75)^2)) \\ &\quad +2\exp(-5(x^2+y^2)) \end{aligned}$$

The highest suitability is reached at four symmetrical points respect to the origin and at the origin. The spatial distribution of the three species is shown in Figure 8.
As in the first case, the mesopredators move towards the sites of higher density of the resource and the top predator is located far enough away from its prey because e_2/e_1 is relatively high. It seems that the richness of the habitat does not induce any change in the distribution patterns. Top predator tends to occupy the areas less densely populated by mesopredators, if e_2/e_1 is high enough.

Resource defense and species distribution

Some species defend themselves by attracting predators from their natural enemies. This is very frequent for instance in plant species, see (Price *et al.*, 1980) and the bibliography cited there. In (Aljbory and Chen, 2018) it has been described 24 species of predators which are attracted by volatiles generated by plants damaged by herbivores. In this paper, the authors raise the question about the effectiveness of predator species in controlling specific insect pests. In the following we analyze numerically the impact on the mesopredator distribution of an increasing predation rate of the top predator when this is attracted by the resource species. To analyze the relationship between the distribution of the mesopredator and the predation rate of a top predator that is attracted to the resource, we use Model (2) which is shown below.

$$\begin{aligned} \frac{\partial u}{\partial t} &= d_0\Delta u+\alpha u(1-\frac{u}{K(x,y)})-\frac{buv}{u+a}, \\ \frac{\partial v}{\partial t} &= d_1\Delta v+\gamma\frac{buv}{u+a}-\frac{cvw}{v+d}-\mu v, \\ \frac{\partial w}{\partial t} &= d_2\Delta w+\beta\frac{cvw}{v+d}-\rho w-\nabla\cdot(\chi_2(u,w)\nabla u). \end{aligned} \tag{12}$$

The sensitivity function is $\chi_2(u,w)=quw$. Thus, the movement of top predators towards the gradient of u is faster the higher its own density or that of the resource.
Initial conditions for the spatial distribution of the resource, the meso-predator and top predator are considered as

$$\begin{aligned} u_0(x,y) &= 2\exp(-(x^2+(y-.9)^2)(1-x^2)^2(1-y^2)^2; \\ v_0(x,y) &= 2\exp(-(x+.9)^2-(y+.9)^2)(1-x^2)^2(1-y^2)^2; \\ w_0(x,y) &= 1.5 \end{aligned}$$

for all $x,y\in\Omega$. The suitability of the habitat of the resource is given by

$$\begin{aligned} K(x,y) &= 2\exp(-5((x+.75)^2+(y-.75)^2)) \\ &\quad +2\exp(-5((x-.75)^2+(y+.75)^2)) \\ &\quad +2\exp(-5((x+.75)^2+(y+.75)^2)) \\ &\quad +2\exp(-5((x-.75)^2+(y-.75)^2)). \end{aligned}$$

Let the parameter values be given by $\alpha=5, a=2.0, b=5.0, d=2.0, \beta=1.0, \gamma=1.0, \mu=0.05, \rho=0.05, d_0=0.1, d_1=1, d_2=1$.
The sensitivity function is $\chi_2(u,w)=quw$. The below simulations are executed for different values of q and c.

It is worth to note that an increment of the predation rate c not necessarily induces an increment on the predator population. In Figure 10 the predation rate is c=1.5, and the predator population is lesser than the population showed in Figure 9 where the predaton rate is $c=1.0$. This is due, in

part, to the weak attraction of the resource on the individual predators, as this allows predators to remain randomly dispersed throughout space preventing the mesopredator population from reaching a level high enough to support a large population of predators. On the other hand, By comparing Figure 10 with Figure 11 we observe that the main effect on the increment of the attraction paremeter q is on the spatial distribution of meso and top predators. For $q = 1.0$ (Figure 11), top predators tend to occupy the places most densely populated by the resource; in contrast, mesopredators occupy the places least densely populated by top predators. However, if the predation rate is large enough, the mesopredator population is depleted and spatial complementarity is lost (see Figure 12). This effect vanishes if he resource's attraction to top predators grows; in fact, for $q = 10$, the separation of top and mesopredators habitats is strengthened for $c = 1$ and all three species reach relatively large populations levels compared to $c = .1$ (see Figure (13-15). The coexistence of the three species requires a proper balance between the rate of predation and the attraction of predators to the resource population. In Figure 14, we observe very low mesopredator population levels and a sharp concentration of top predators around the areas most populated by mesopredators.

4 CONCLUSIONS

With the aim to analyze the rol of migration and defensive mechanisms of the prey, in this work two variations of a tritrophic model have been considered. According to Table (1), if the three species remain in the same location (Model 4 without diffusion), top predator would become extinct since only the equliibrium point P_3 is stable. In the first case, where a top predator is an active-search hunter it is assumed that as prey density increases, searching intensity decreases (Model (1) with $\chi_1(v,w) = e_1 w - e_2 v$). Numerical simulations show that all three species coexist and both resource and prey tend to be concentrated around sites $(x^*, y^*) \in \Omega$ where resource suitability is greatest; that is, sites (x^*, y^*) where the carrying capacity $K(x^*, y^*)$ is the maximum. The spatial distribution of predator depends on the defensive capacity of the prey; for e_2/e_1 low enough, predators and prey have a similar distribution (see Figures 6, 5). However, if e_2/e_1 reaches a large enough level, the resource and prey populations share the same space, but the predator occupies the locations less populated by prey(see Figures 2, 3, 4). Hence, our numerical simulations provide evidence that migration favors coexistence and behavioral characteristics, such as a defense mechanism, can impact the spatial distribution of species. Furthermore, we find that the distribution of prey follows a pattern similar to that of the resource, which tends to be distributed near the places of greatest suitability. The spatial distribution is topic which has been analyzed from a diverse points of interest. For instance, the cost of a defense mechanism has been considered in (Wang *et al.*, 2017) where the authors analyze how this cost impact on pattern distribution of predators and preys. The role of predators on the spatial distribution has been studied from a experimental point of view in (Livingston *et al.*, 2017), where preys do not present a defense against predators. They found that was not the patch type but the distribution of predators that most strongly predicted the composition of the prey community. The effect of diffussion on the spatial distribution has beeen analyzed in (Kumari, 2013) .

A second point of interest in this work is how the attraction of enemies of my enemies influences the dynamics of a community. In some cases, the attraction activity is caused by volatiles emitted by the resource organisms. We have analyzed this question with the Model (2) where the predator moves toward the resource gradient according to the sensivity function $\chi_2(u,w) = quw$; that is, the higher the population density of the resource or the predator, the greater the tendency of the predator to move towards the resource. From Figures 9 and 15, we observe that a high attraction favors a greater concentration of both the top predators and the resource around the patches with the highest carrying capacity of the resource; as the predation pressure decreases in the other patches, they are occupied by the mesopredator. This phenomenon becomes more acute if predation increases (see Figure 14). It is also apparent that the larger q the greater the concentration of the populations. A fact that seems counterintuitive is that an increase in the predation rate does not necessarily lead to lower mesopredator densities; this is shown in Figures 9 and 10, where even we observe a similar pattern of the spatial distribution of the three species, the population levels of the mesopredator are higher in 10 with $c = 1.5$ than in 9, ($c = 1.0$); Possibly, this is a consequence of the fact that the greater the predation, the lower the population of mesopredators that arrive in the areas of greatest productivity of the resource. The general findings shown in this paper could be useful to the study of the biological factors that impact the spatial distribution of species.

doi: 10.58560/rmmsb.v03.n02.023.08

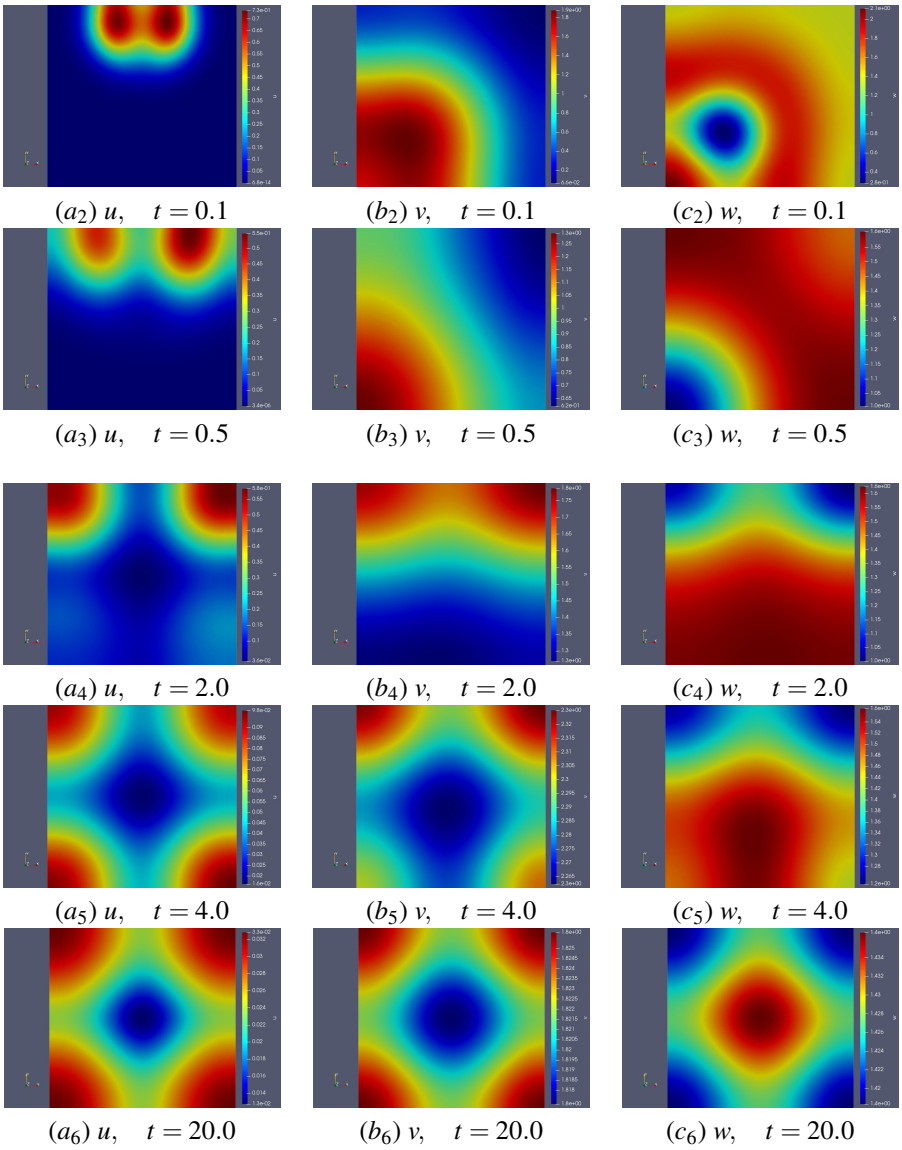

$(a_2)\ u, \quad t = 0.1$ $(b_2)\ v, \quad t = 0.1$ $(c_2)\ w, \quad t = 0.1$

$(a_3)\ u, \quad t = 0.5$ $(b_3)\ v, \quad t = 0.5$ $(c_3)\ w, \quad t = 0.5$

$(a_4)\ u, \quad t = 2.0$ $(b_4)\ v, \quad t = 2.0$ $(c_4)\ w, \quad t = 2.0$

$(a_5)\ u, \quad t = 4.0$ $(b_5)\ v, \quad t = 4.0$ $(c_5)\ w, \quad t = 4.0$

$(a_6)\ u, \quad t = 20.0$ $(b_6)\ v, \quad t = 20.0$ $(c_6)\ w, \quad t = 20.0$

Figure 2: Evolution of the spatial distribution of the three species. $e_1 = 1.0, e_2 = 1.0$

doi: 10.58560/rmmsb.v03.n02.023.08

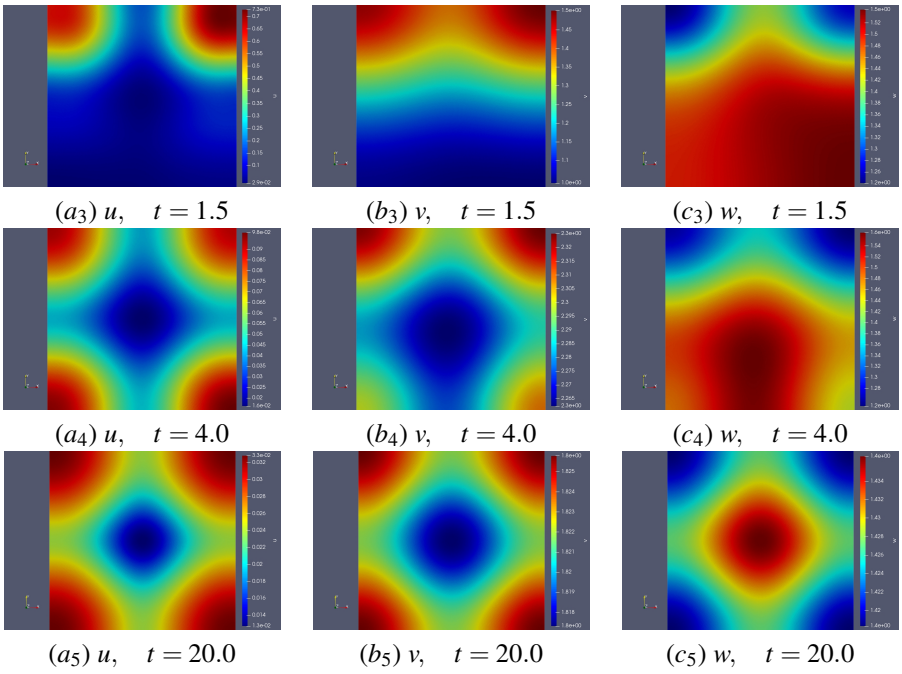

$(a_3)\ u, \quad t = 1.5$ $(b_3)\ v, \quad t = 1.5$ $(c_3)\ w, \quad t = 1.5$

$(a_4)\ u, \quad t = 4.0$ $(b_4)\ v, \quad t = 4.0$ $(c_4)\ w, \quad t = 4.0$

$(a_5)\ u, \quad t = 20.0$ $(b_5)\ v, \quad t = 20.0$ $(c_5)\ w, \quad t = 20.0$

Figure 3: Evolution of the spatial distribution of the three species. $e_1 = 1.0, e_2 = 2.0$

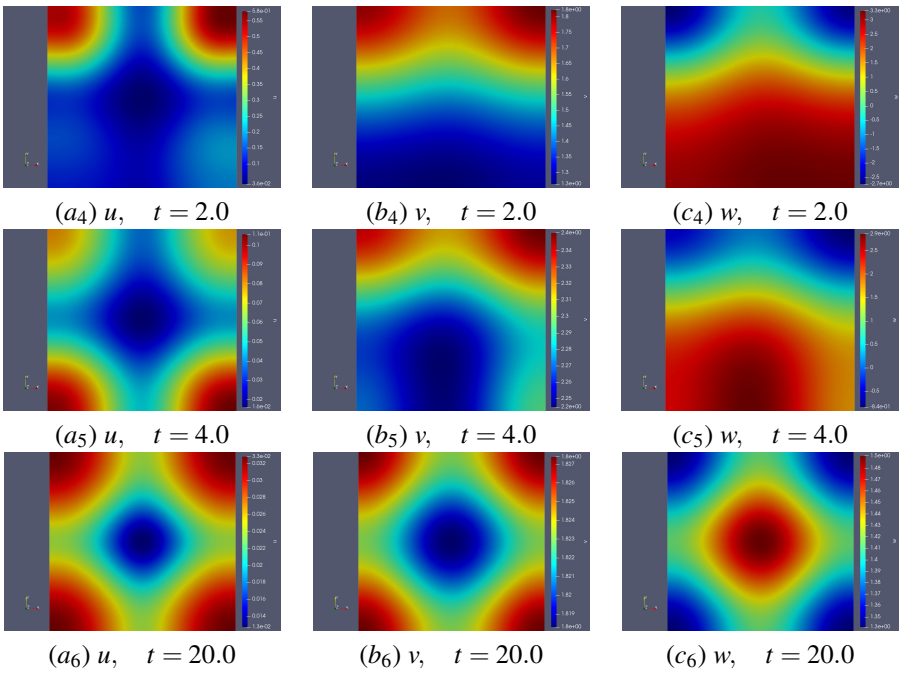

$(a_4)\ u, \quad t = 2.0$ $(b_4)\ v, \quad t = 2.0$ $(c_4)\ w, \quad t = 2.0$

$(a_5)\ u, \quad t = 4.0$ $(b_5)\ v, \quad t = 4.0$ $(c_5)\ w, \quad t = 4.0$

$(a_6)\ u, \quad t = 20.0$ $(b_6)\ v, \quad t = 20.0$ $(c_6)\ w, \quad t = 20.0$

Figure 4: Evolution of the spatial distribution of the three species. $e_1 = 1.0, e_2 = 10.0$

doi: 10.58560/rmmsb.v03.n02.023.08

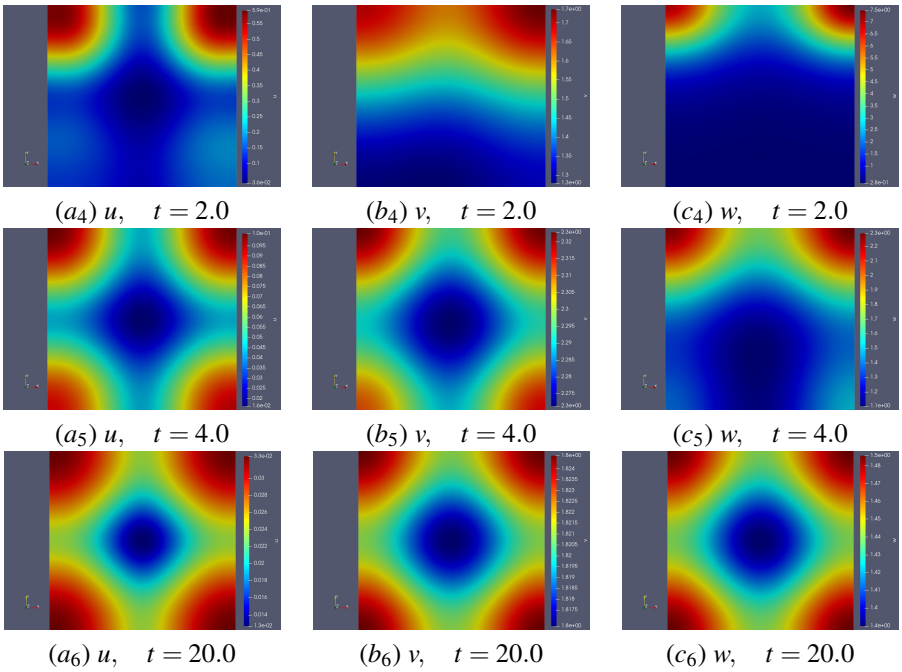

$(a_4)\ u, \quad t = 2.0$ $(b_4)\ v, \quad t = 2.0$ $(c_4)\ w, \quad t = 2.0$

$(a_5)\ u, \quad t = 4.0$ $(b_5)\ v, \quad t = 4.0$ $(c_5)\ w, \quad t = 4.0$

$(a_6)\ u, \quad t = 20.0$ $(b_6)\ v, \quad t = 20.0$ $(c_6)\ w, \quad t = 20.0$

Figure 5: Evolution of the spatial distribution of the three species. $e_1 = 10.0, e_2 = 1.0$

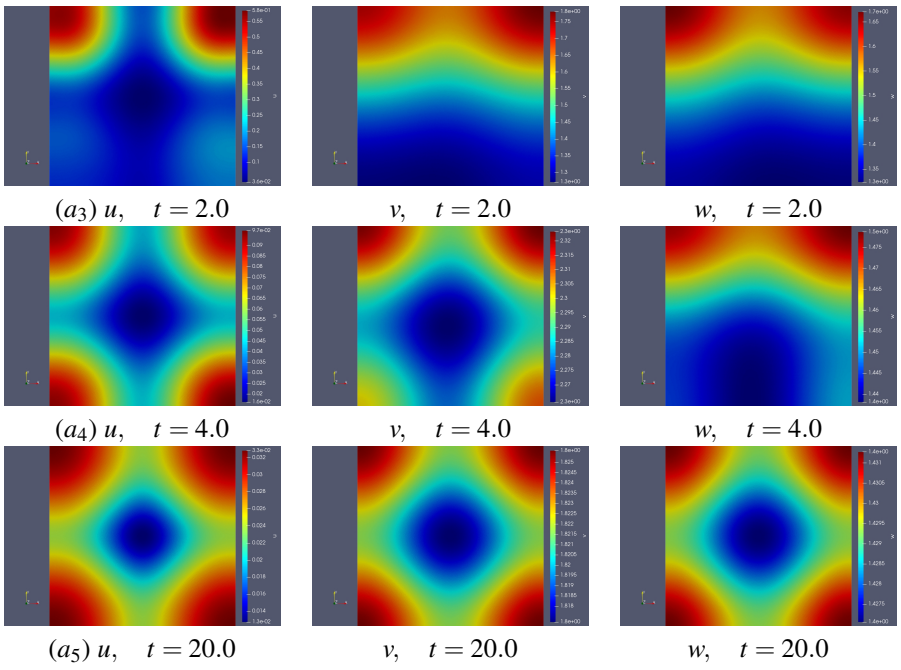

$(a_3)\ u, \quad t = 2.0$ $v, \quad t = 2.0$ $w, \quad t = 2.0$

$(a_4)\ u, \quad t = 4.0$ $v, \quad t = 4.0$ $w, \quad t = 4.0$

$(a_5)\ u, \quad t = 20.0$ $v, \quad t = 20.0$ $w, \quad t = 20.0$

Figure 6: Evolution of the spatial distribution of the three species. $e_1 = 1.0, e_2 = 0.5$

doi: 10.58560/rmmsb.v03.n02.023.08

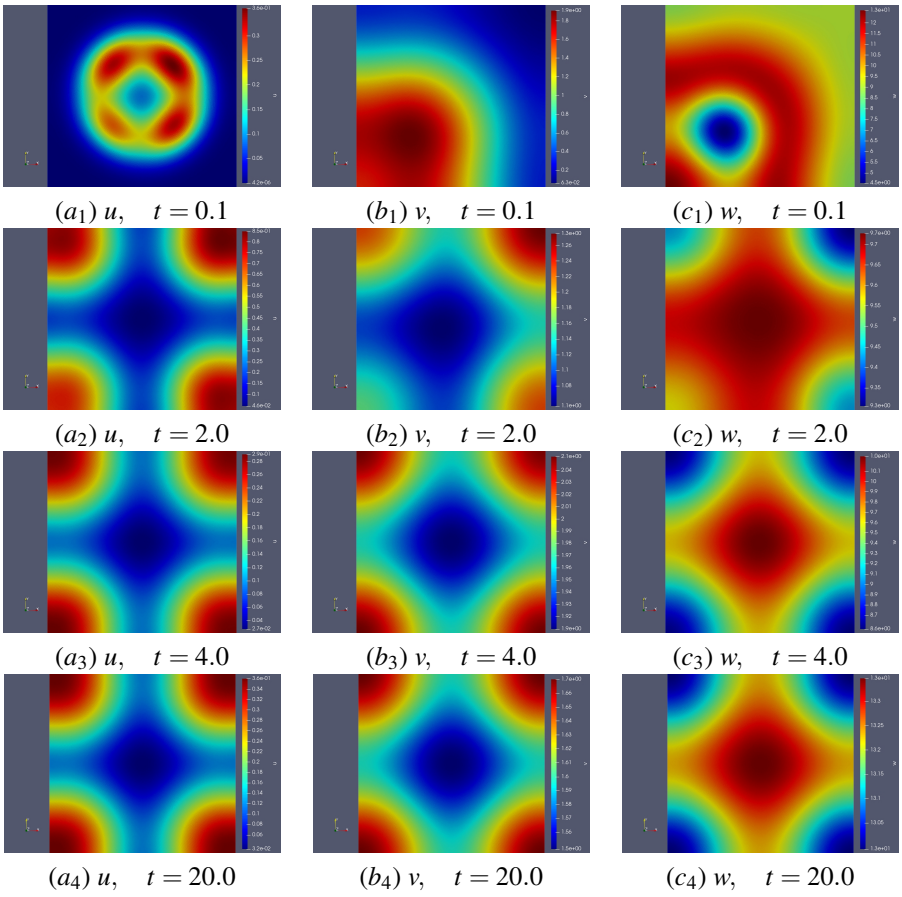

$(a_1)\ u, \quad t = 0.1$ $(b_1)\ v, \quad t = 0.1$ $(c_1)\ w, \quad t = 0.1$

$(a_2)\ u, \quad t = 2.0$ $(b_2)\ v, \quad t = 2.0$ $(c_2)\ w, \quad t = 2.0$

$(a_3)\ u, \quad t = 4.0$ $(b_3)\ v, \quad t = 4.0$ $(c_3)\ w, \quad t = 4.0$

$(a_4)\ u, \quad t = 20.0$ $(b_4)\ v, \quad t = 20.0$ $(c_4)\ w, \quad t = 20.0$

Figure 7: Evolution of the spatial distribution of the three species.

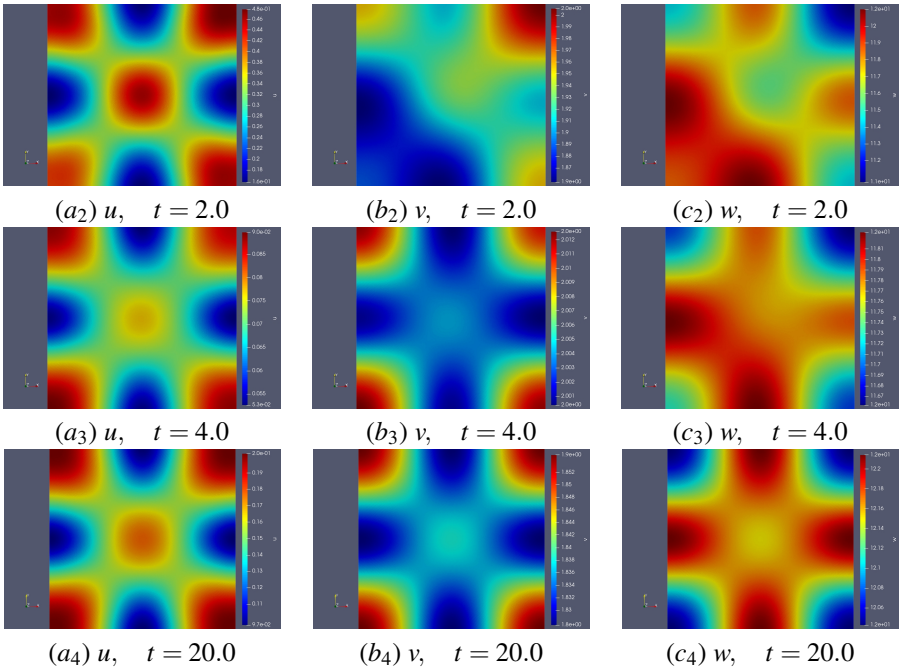

$(a_2)\ u, \quad t = 2.0$ $(b_2)\ v, \quad t = 2.0$ $(c_2)\ w, \quad t = 2.0$

$(a_3)\ u, \quad t = 4.0$ $(b_3)\ v, \quad t = 4.0$ $(c_3)\ w, \quad t = 4.0$

$(a_4)\ u, \quad t = 20.0$ $(b_4)\ v, \quad t = 20.0$ $(c_4)\ w, \quad t = 20.0$

Figure 8: Evolution of the spatial distribution of the three species. The suitability of resource habitat is given by (12)

.

doi: 10.58560/rmmsb.v03.n02.023.08

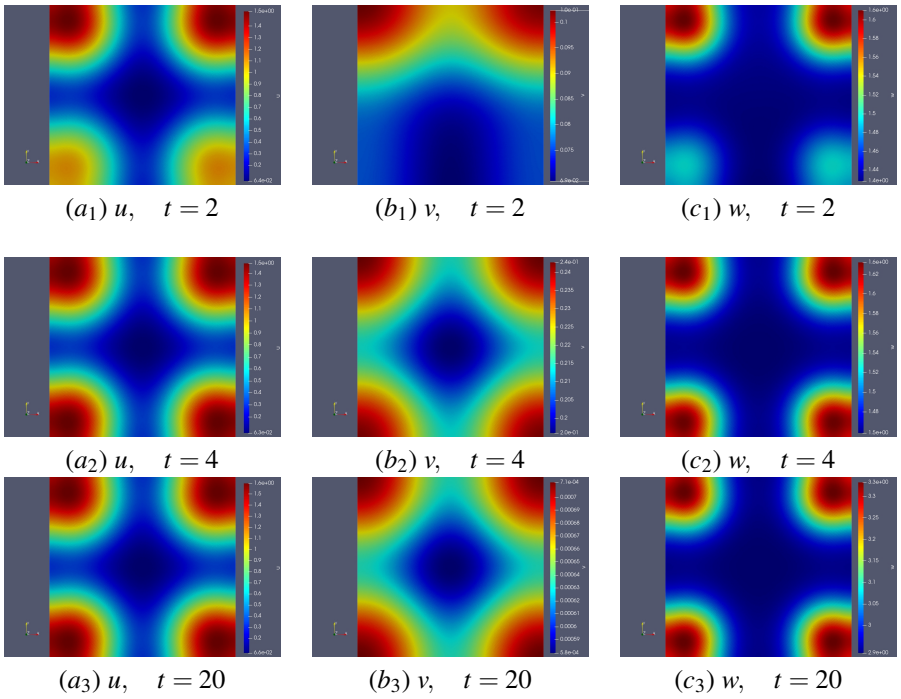

$(a_1)\ u, \quad t = 2$ $(b_1)\ v, \quad t = 2$ $(c_1)\ w, \quad t = 2$

$(a_2)\ u, \quad t = 4$ $(b_2)\ v, \quad t = 4$ $(c_2)\ w, \quad t = 4$

$(a_3)\ u, \quad t = 20$ $(b_3)\ v, \quad t = 20$ $(c_3)\ w, \quad t = 20$

Figure 9: *Contour plots* of time evolution of the resource u, mesopredador v and top predador w at different times. $q = 0.1$, $c = 1.0$

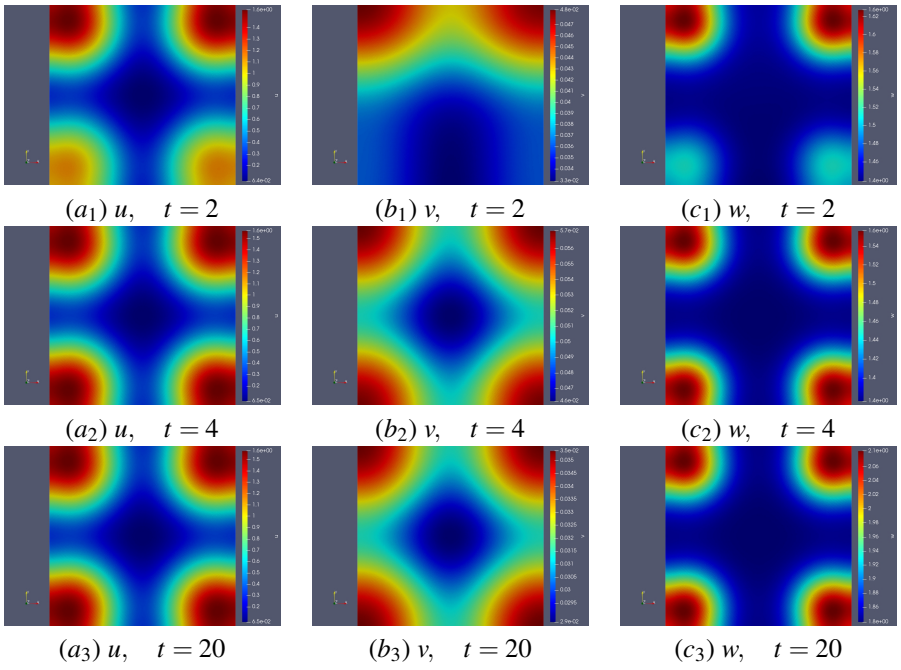

$(a_1)\ u, \quad t = 2$ $(b_1)\ v, \quad t = 2$ $(c_1)\ w, \quad t = 2$

$(a_2)\ u, \quad t = 4$ $(b_2)\ v, \quad t = 4$ $(c_2)\ w, \quad t = 4$

$(a_3)\ u, \quad t = 20$ $(b_3)\ v, \quad t = 20$ $(c_3)\ w, \quad t = 20$

Figure 10: *Contour plots* of time evolution of the resource u, mesopredador v and top predador w at different times. $q = 0.1$, $c = 1.5$

doi: 10.58560/rmmsb.v03.n02.023.08

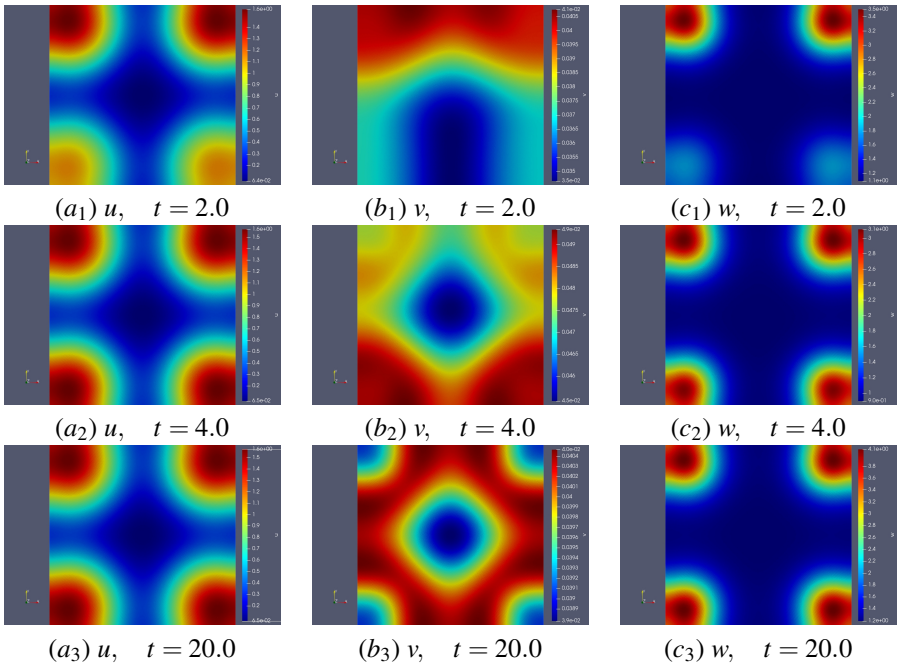

Figure 11: *Contour plots* of time evolution of the resource u, mesopredador v and top predador w at different times. $q = 1.0$, $c = 1.5$

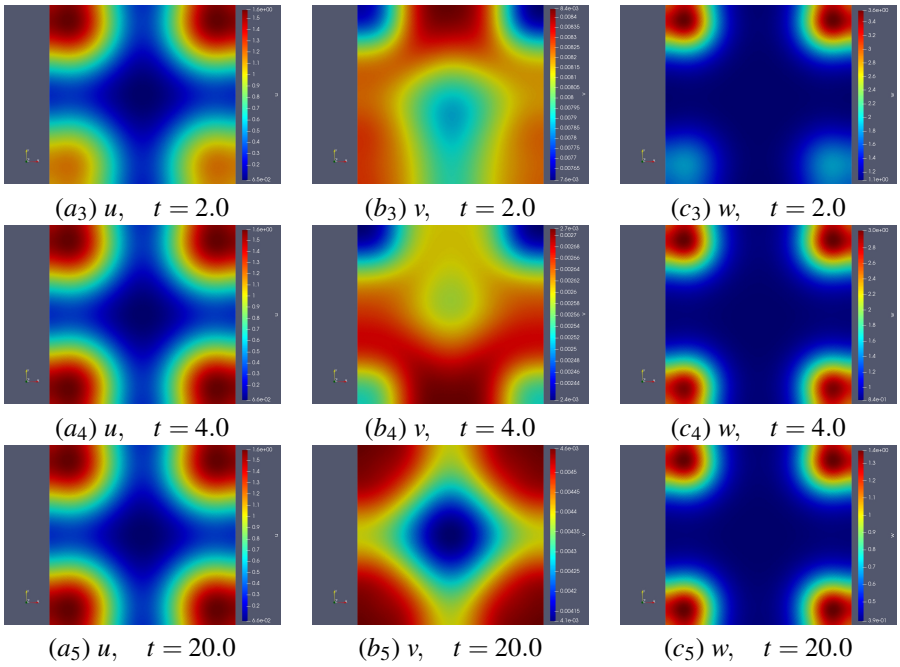

Figure 12: *Contour plots* of time evolution of the resource u, mesopredador v and top predador w at different times. $q = 1.0$, $c = 2.5$

doi: 10.58560/rmmsb.v03.n02.023.08

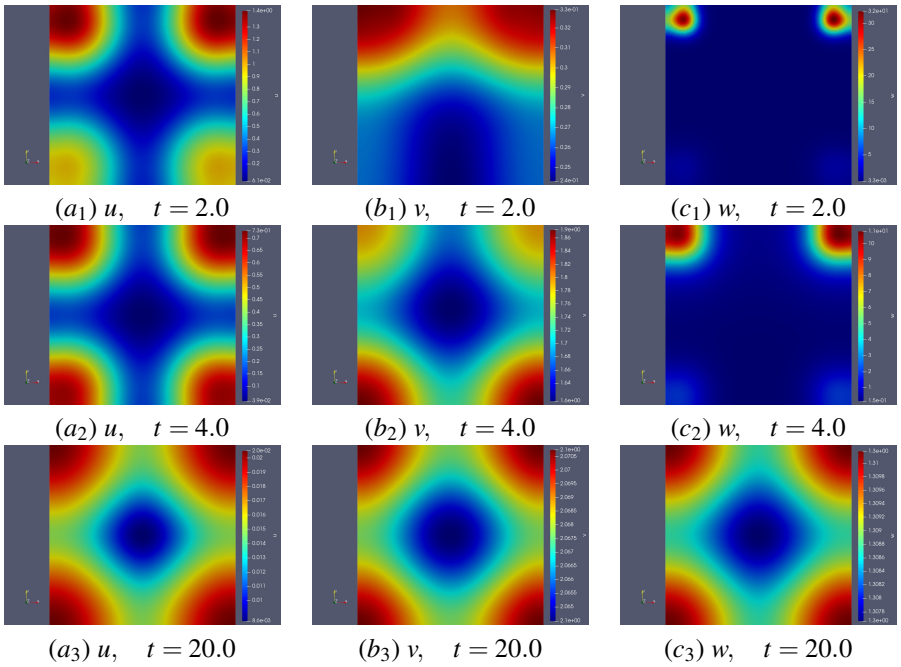

Figure 13: *Contour plots* of time evolution of the resource u, mesopredador v and top predador w at different times. $q = 10.0$, $c = .1$

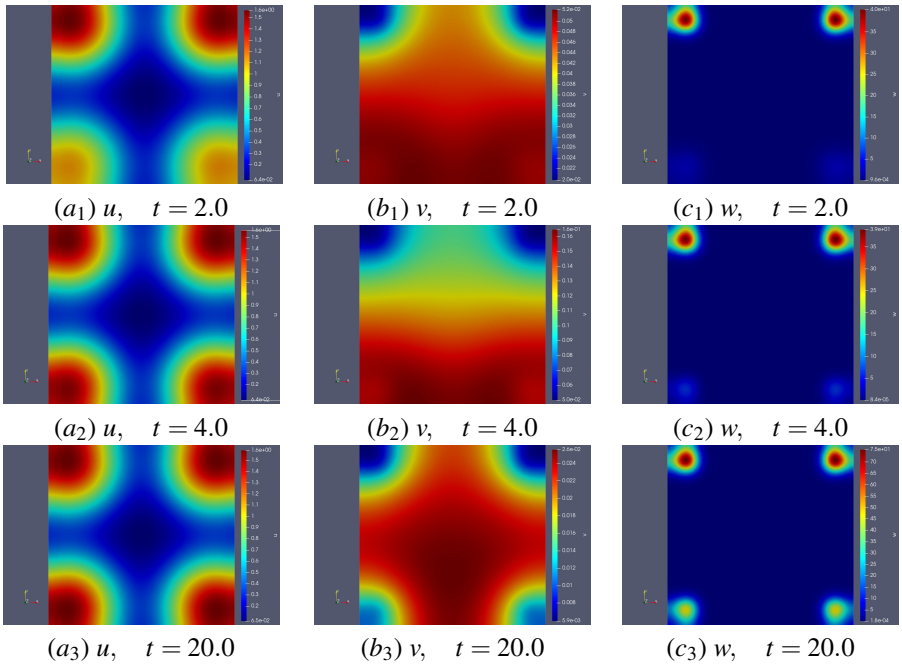

Figure 14: *Contour plots* of time evolution of the resource u, mesopredador v and top predador w at different times. $q = 10.0$, $c = 1.5$

doi: 10.58560/rmmsb.v03.n02.023.08

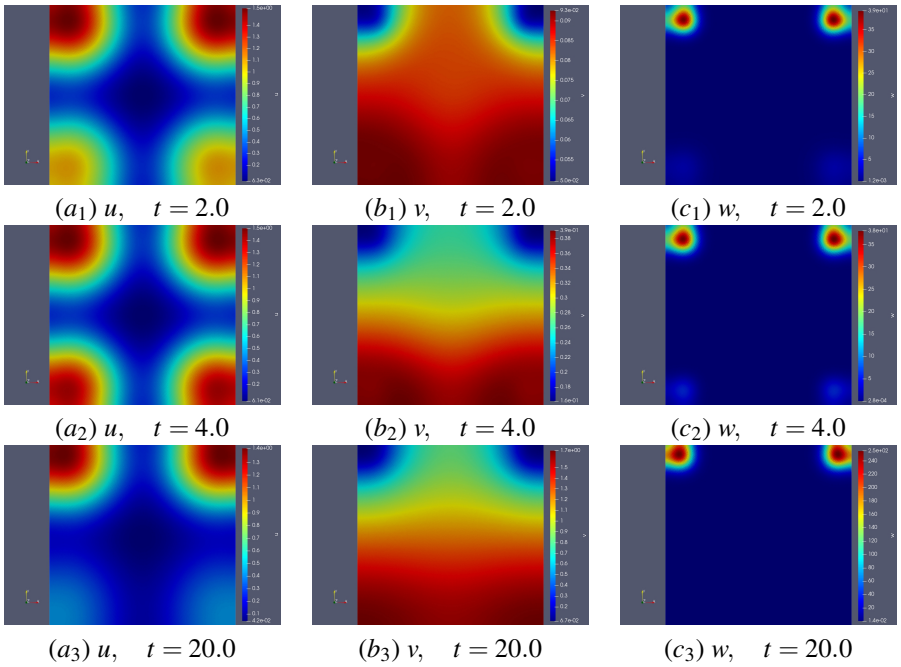

$(a_1)\ u, \quad t = 2.0$ $(b_1)\ v, \quad t = 2.0$ $(c_1)\ w, \quad t = 2.0$

$(a_2)\ u, \quad t = 4.0$ $(b_2)\ v, \quad t = 4.0$ $(c_2)\ w, \quad t = 4.0$

$(a_3)\ u, \quad t = 20.0$ $(b_3)\ v, \quad t = 20.0$ $(c_3)\ w, \quad t = 20.0$

Figure 15: *Contour plots* of time evolution of the resource u, mesopredador v and top predador w at different times. $q = 10.0$, $c = 1.0$

doi: 10.58560/rmmsb.v03.n02.023.08

SUPPORT

- G. González thanks PAPIIT-UNAM IN114319 for academic and financial support. We thank to PAPIIT IA203922.
- N. Anaya also thankful to CONACYT for the grant a the postdoctotal fellowship at Facultad de Ciencias, Universidad Nacional Autónoma de México(UNAM) in 2018-2020.

CONTRIBUTION OF THE AUTHORS (CREDIT)

The three authors contributed equally in

- Conceptualization
- Formal Analysis
- Investigation
- Writing – original draft

A APPENDIX

SPATIAL DISCRETIZATION

Variational formulation

We consider a general reaction-diffusion problem with Neumann boundary conditions

$$\begin{aligned} -\Delta u + \mu u &= f \quad \text{en } \Omega && (13)\\ u(x,0) &= u_0(x) \quad \text{en } \Omega && (14)\\ \partial_n u(x,t) &= 0 \quad \text{en } \partial\Omega && (15) \end{aligned}$$

where function $f \in C^0(\Omega)$ is regular, $\mu \in \mathbb{R}$. As it is usual $\partial_n u = \nabla u \cdot \mathbf{n}$, where $\mathbf{n}$ is the exterior normal vector to $\partial\Omega$.

A classic solution of the above problem (13)–(15) is a function $u : \bar{\Omega} \mapsto \mathbb{R}$, $u \in C^2(\bar{\Omega})$ which satisfies (13)–(15). In order to facilitate the search of u we reformulate the problem to find a equivalent solution.

Let $v \in C^2(\bar{\Omega})$. Multiplying (13) by v it is obtained

$$-v\Delta u + \mu uv = fv$$

Integrating on Ω

$$-\int_\Omega v\Delta u \, d\Omega + \mu \int_\Omega uv \, d\Omega = \int_\Omega fv \, d\Omega \qquad (16)$$

Applying the Green Theorem

$$\int_\Omega \nabla u \cdot \nabla v \, d\Omega - \int_{\partial\Omega} (\nabla u \cdot \mathbf{n}) v \, dS + \mu \int_\Omega uv \, d\Omega = \int_\Omega fv \, d\Omega. \qquad (17)$$

Since $\partial_n u = 0$ for $x \in \partial\Omega$, we have

$$\int_\Omega \nabla u \cdot \nabla v \, d\Omega + \mu \int_\Omega uv \, d\Omega = \int_\Omega fv \, d\Omega. \qquad (18)$$

This expression is known as variational formulation of the problem (13)–(15), see (Vidar, 2007). Notice that in (18) it is only required that $u, v \in C^1(\bar{\Omega})$. Furthermore, they can even be just continuous.

Discretization Finite Element Method

Let $H^k(\Omega)$ a Sobolev space and $C^1(0,T,C^2(\bar{\Omega}))$ is the space of continuously differentiable functions from $[0,T]$ on $C^2(\bar{\Omega})$. Ω_h is a polygonal approximation of Ω. We consider a mesh T_h of Ω_h consisting of convex elements $E_i \in T_h$, $i \in I$, $I \subset \mathbb{N}$.

Let $\{\varphi_j(x,y)\}_{1\le j\le N}$ be a base of V_h

$$\begin{aligned} u_h(x,y,t) &= \sum_{j=1}^{N} u_i(t)\varphi_j(x,y)\\ v_h(x,y,t) &= \sum_{j=1}^{N} v_i(t)\varphi_j(x,y)\\ w_h(x,y,t) &= \sum_{j=1}^{N} w_j(t)\varphi_j(x,y) \end{aligned}$$

$x, y \in \Omega$, $0 \le t \le T$. The basis $\varphi_j(x,y)$ are compact support functions and we use the usual linear elements $P1$ defined on triangles.

Parameter h represents the size of element E_i of mesh T_h and is defined as

$$h = \max_{E_i \in T_h} \operatorname{diam}(E_i),$$

as $h \mapsto 0$, space V_h is closer to $H^k(\Omega)$.

SEMI-DISCRETIZATION OF TIME

Let

$$0 = t_0 < t_1 < \cdots t_N = T,$$

a partition of the interval $[0,T]$ with constant step $dt = t_{m+1} - t_m$ for all $m \in \{0,\ldots,N-1\}$. The derivative with respect to time is approximated using forward finite differences

$$u_t = \frac{u^{m+1}-u^m}{dt}, \quad v_t = \frac{v^{m+1}-v^m}{dt}, \quad w_t = \frac{w^{m+1}-w^m}{dt}$$

where $u^m = u(x,t_m), v^m = v(x,t_m), w^m = w(x,t_m)$.

By substituting the above approximation in Model (1) we obtain that

$$\begin{aligned} u^{m+1} &= u^m + dt\cdot d_0\Delta u^{m+1} + dt\cdot \alpha u^{m+1}(1-\frac{u^{m+1}}{K(x,y)})\\ &\quad -dt\cdot\frac{bu^{m+1}v^{m+1}}{u^{m+1}+a},\\ v^{m+1} &= v^m + dt\cdot d_1\Delta v^{m+1} + dt\cdot\gamma\frac{bu^{m+1}v^{m+1}}{u^{m+1}+a}\\ &\quad -dt\cdot\frac{cv^{m+1}w^{m+1}}{v^{m+1}+d} - \mu v^{m+1} \qquad (19)\\ w^{m+1} &= w^m + dt\cdot d_2\Delta w^{m+1} + dt\cdot\beta\frac{cv^{m+1}w^{m+1}}{v^{m+1}+d}\\ &\quad -dt\cdot\rho w^{m+1} - dt\cdot\nabla\cdot(\chi_2(v^{m+1},w^{m+1})\nabla v^{m+1}). \end{aligned}$$

This is the Implicit Euler Method which depends on both $(x,y) \in \Omega$ for each element E_i and the boundary conditions

$$\nabla u^{m+1}\cdot\mathbf{n}=0,\ \nabla v^{m+1}\cdot\mathbf{n}=0,\ \nabla w^{m+1}\cdot\mathbf{n}=0,\quad m\geq 0. \quad (20)$$

From the initial values u_0, v_0, and w_0, we compute the next iterations $(u_1,v_1,w_1),\ \ldots,(u_N,v_N,w_N)$. The system (19) is solved by FEM, assuming that $u_0,v_0,w_0\in C^2(\bar{\Omega})$, see (Douglas and Dupont, 1970). To avoid some complications which arise from the nonlinearity involved in (19), the terms corresponding to temporal variation are solved using a semi-implicit Runge-Kutta method of second order. The two steps of this computational process are depicted in the following. First, the right side of equations (1) are rewritten as

$$\begin{aligned} F(u,v,w) &= d_0\Delta u+\alpha u(1-\frac{u}{K(x,y)})-\frac{buv}{u+a},\\ G(u,v,w) &= d_1\Delta v+\gamma\frac{buv}{u+a}-\frac{cvw}{v+d}-\mu v, \quad (21)\\ H(u,v,w) &= d_2\Delta w+\beta\frac{cvw}{v+d}-\rho w-\nabla\cdot(\chi_2(v,w)\nabla v). \end{aligned}$$

The first step of the RK–method of second order consists in an one Euler step computed at central point of each time interval.

$$u^{m+1/2} = u^m+\frac{dt}{2}\cdot F(u^m,v^m,w^m) \quad (22)$$

$$v^{m+1/2} = v^m+\frac{dt}{2}\cdot G(u^m,v^m,w^m) \quad (23)$$

$$w^{m+1/2} = w^m+\frac{dt}{2}\cdot H(u^m,v^m,w^m) \quad (24)$$

In the second step, computations are made at time $m+1$ like

$$u^{m+1} = u^m+dt\cdot F(u^{m+1/2},v^{m+1/2},w^{m+1/2}) \quad (25)$$

$$v^{m+1} = v^m+dt\cdot G(u^{m+1/2},v^{m+1/2},w^{m+1/2}) \quad (26)$$

$$w^{m+1} = w^m+dt\cdot H(u^{m+1/2},v^{m+1/2},w^{m+1/2}) \quad (27)$$

Now we considered the diffusion in an implicit form, then the schema becomes a semi-implicit one. For each step, the equations are solved by applying the FEM Galerkin-Ritz method described above.The same scheme of discretization is applied to Model (2).

SUPPORT

Research fully (or partially) supported by:

- PAPIIT IA203922

REFERENCES

Ai, S., Du, Y. and Peng, R. (2017) 'Traveling waves for a generalized holling–tanner predator–prey model'. *Journal of Differential Equations*, 263(11), pp. 7782–7814.

Aljbory, Z. and Chen, M.S. (2018) 'Indirect plant defense against insect herbivores: a review'. *Indirect plant defense against insect herbivores: a review*, 25(1), pp. 2–23.

Amann, H. (1990) 'Dynamic theory of quasilinear parabolic equations. ii: Reaction–difussion systems'. *Differential Integral Equations*, 3, pp. 13–15.

Buonomo, B., Gainnino, F., Saussure, S. and Venturino, E. (2019) 'Effects of limited volatiles release by plants in tritrophic interactions'. *Mathematical Biosciences and Engineering*, 165(5), pp. 3331–3344.

Douglas, J.J. and Dupont, T. (1970) 'Galerkin methods for parabolic equations'. *SIAM Journal on Numerical Analysis*, 7(4), pp. 575–626.

Dumbacher, J.P. and Pruett-Jones, S. (1996) 'Avian chemical defense'. *Current ornithology*, pp. 137–174.

Eisner, T., Eisner, M., Rossini, C., Iyengar, V.K., Roach, B.L., Benedikt, E. and Meinwald, J. (2000) 'Chemical defense against predation in an insect egg'. *Proceedings of the National Academy of Sciences*, 97(4), pp. 1634–1639.

Fattorini, D., Notti, A., Nigro, M. and Regoli, F. (2010) 'Hyperaccumulation of vanadium in the antarctic polychaete perkinsiana littoralis as a natural chemical defense against predation'. *Environmental Science and Pollution Research*, 17, pp. 220–228.

Han, R. and Dai, B. (2017) 'Spatiotemporal dynamics and spatial pattern in a diffusive intraguild predation model with delay effect'. *Applied Mathematics and Computation*, 312, pp. 177–201.

Haskell, E.C. and Bell, J. (2020) 'Pattern formation in a predator-mediated coexistence model with prey-taxis'. *Discrete and Continuous Dynamical Systems-B*, 25(8), pp. 2895–2921.

Hecht, F. (2012) 'New development in freefem++'. *Journal of numerical mathematics*, 20(3-4), pp. 251–266.

Henry, D. (2006) *Geometric theory of semilinear parabolic equations*, vol. 840. Springer.

Iino, Y. and Yoshida, K. (2009) 'Parallel use of two behavioral mechanisms for chemotaxis in caenorhabditis elegans'. *Journal of Neuroscience*, 29(17), pp. 5370–5380.

Ioannou, C.C. and Krause, J. (2008) 'Searching for prey: the effects of group size and number'. *Animal Behaviour*, 75(4), pp. 1383–1388.

Kessler, A. and Baldwin, I.T. (2001) 'Defensive function of herbivore-induced plant volatile emissions in nature'. *Science*, 291(5511), pp. 2141–2144.

Kolmogorov, A. (1937) 'Étude de l'équation de la diffusion avec croissance de la quantité de matière et son application à un problème biologique'. *Moscow Univ. Bull. Math.*, 1, pp. 1–25.

Kumari, N. (2013) 'Pattern formation in spatially extended tritrophic food chain model systems: generalist versus specialist top predator'. *International Scholarly Research Notices*, 2013.

Livingston, G., Fukumori, K., Provete, D.B., Kawachi, M., Takamura, N. and Leibold, M.A. (2017) 'Predators regulate prey species sorting and spatial distribution in microbial landscapes'. *Journal of Animal Ecology*, 86(3), pp. 501–510.

Matz, C., Webb, J.S., Schupp, P.J., Phang, S.Y., Penesyan, A., Egan, S., Steinberg, P. and Kjelleberg, S. (2008) 'Marine biofilm bacteria evade eukaryotic predation by targeted chemical defense'. *PloS one*, 3(7), p. e2744.

Osorio-Olvera, L. and Falconi, J.S.M. (2019) 'On population abundance and niche structure'. *Ecography*, 42(8), pp. 1415–1425.

Pereira, R.C., Donato, R., Teixeira, V.L. and Cavalcanti, D.N. (2000) 'Chemotaxis and chemical defenses in seaweed susceptibility to herbivory'. *Revista Brasileira de Biologia*, 60, pp. 405–414.

Polis, G.A. and Holt, R.D. (1992) 'Intraguild predation: the dynamics of complex trophic interactions'. *Trends in ecology & evolution*, 7(5), pp. 151–154.

Price, P.W., Bouton, C.E., Gross, P., McPheron, B.A., Thompson, J.N. and Weis, A.E. (1980) 'Interactions among three trophic levels: influence of plants on interactions between insect herbivores and natural enemies'. *Annual review of Ecology and Systematics*, 11(1), pp. 41–65.

Raina, J.B., Fernandez, V., Lambert, B., Stocker, R. and Seymour, J.R. (2019) 'The role of microbial motility and chemotaxis in symbiosis'. *Nature Reviews Microbiology*, 17(5), pp. 284–294.

Ross, T.C. and Winterhalder, B. (2015) 'Sit-and-wait versus active-search hunting: A behavioral ecological model of optimal search mode'. *Journal of Theoretical Biology*, 387, pp. 76–87.

Skellam, J.G. (1951) 'Random dispersal in theoretical populations'.

Biometrika, 38(1/2), pp. 196–218.

Song, D., Song, Y. and Li, C. (2020) 'Stability and turing patterns in a predator–prey model with hunting cooperation and allee effect in prey population'. *International Journal of Bifurcation and Chaos*, 30(09), p. 2050137.

Tello, J.I. and Wrzosek, D. (2016) 'Predator–prey model with diffusion and indirect prey-taxis'. *Mathematical Models and Methods in Applied Sciences*, 26(11), pp. 2129–2162.

Venturino, E. and Petrovskii, S. (2013) 'Spatiotemporal behavior of a prey–predator system with a group defense for prey'. *Ecological Complexity*, 14, pp. 37–47.

Vidar, T. (2007) *Galerkin finite element methods for parabolic problems*, vol. 25. Springer Science & Business Media.

Wang, K., Wang, Q. and Yu, F. (2017) 'Stationary and time periodic patterns of two-predator and one-prey systems with prey-taxis'. *Discrete and Continuous Dynamical Systems - A*, 1(37), pp. 505–543.

Yang, F. and Fu, S. (2008) 'Global solutions for a tritrophic food chain model with diffusion'. *The Rocky Mountain Journal of Mathematics*, pp. 1785–1812.

Yoshimizu, T., Hisashi, H.S., Ashida, K., Hotta, K. and Oka, K. (2018) 'Effect of interactions among individuals on the chemotaxis behaviours of caenorhabditis elegans'. *Journal of Experimental Biology*, 221(11), p. jeb182790.

Recommended Citation: Anaya, N. *et al.* (2023). *'Estrategias de búsqueda y defensa inducidas por quimiotaxis en un sistema tritrófico'*. Rev. model. mat. sist. biol. 3(2), e23R05, doi:10.58560/rmmsb.v03.n02.023.08

Support: PAPIIT IA203922